

In conclusion, the present study suggests that PEG-IFN therapy after curative treatment of HCC can improve the prognosis and inhibit the recurrence of HCV-related HCC. This work involved a nonrandomized study, so further prospective studies with a larger number of cases are required to reach firm conclusions.

Conflict of interest No author has any conflict of interest.

References

1. Tsukuma H, Hiyama T, Tanaka S et al (1993) Risk factors for hepatocellular carcinoma among patients with chronic liver disease. *N Engl J Med* 328:1797–1801
2. Takano S, Yokosuka O, Imazeki F et al (1995) Incidence of hepatocellular carcinoma in chronic hepatitis B and C: a prospective study of 251 patients. *Hepatology* 21:650–655
3. Shiratori Y, Shiina S, Imamura M et al (1995) Characteristic difference of hepatocellular carcinoma between hepatitis B- and C-viral infection in Japan. *Hepatology* 22:1027–1033
4. Ikeda K, Saitoh S, Tsubota A et al (1993) Risk factors for tumor recurrence and prognosis after curative resection of hepatocellular carcinoma. *Cancer (Phila)* 71:19–25
5. Tateishi R, Shiina S, Teratani T et al (2005) Percutaneous radiofrequency ablation for hepatocellular carcinoma. An analysis of 1000 cases. *Cancer (Phila)* 103:1201–1209
6. Mazziotti A, Grazi GL, Cavallari A (1998) Surgical treatment of hepatocellular carcinoma on cirrhosis: a Western experience. *Hepatogastroenterology* 45(suppl 3):1281–1287
7. Livraghi T, Goldberg SN, Lazzaroni S et al (1999) Small hepatocellular carcinoma: treatment with radio-frequency ablation versus ethanol injection. *Radiology* 210:655–661
8. Kubo S, Nishiguchi S, Shuto T et al (1999) Effects of continuous hepatitis with persistent hepatitis C viremia on outcome after resection of hepatocellular carcinoma. *Jpn J Cancer Res* 90:162–170
9. Kumada T, Nakano S, Takeda I et al (1997) Patterns of recurrence after initial treatment in patients with small hepatocellular carcinoma. *Hepatology* 25:87–92
10. Shimada M, Takenaka K, Gion T et al (1996) Prognosis of recurrent hepatocellular carcinoma: a 10-year surgical experience in Japan. *Gastroenterology* 111:720–726
11. Nagasue N, Uchida M, Makino Y et al (1993) Incidence and factors associated with intrahepatic recurrence following resection of hepatocellular carcinoma. *Gastroenterology* 105:488–494
12. Davis GL, Balart LA, Schiff ER et al (1989) Treatment of chronic hepatitis C with recombinant interferon alfa. A multicenter randomized, controlled trial. Hepatitis Interventional Therapy Group. *N Engl J Med* 321:1501–1506
13. Di Bisceglie AM, Martin P, Kassianides C et al (1989) Recombinant interferon alfa therapy for chronic hepatitis C. A randomized, double-blind, placebo-controlled trial. *N Engl J Med* 321:1506–1510
14. Nishiguchi S, Kuroki T, Nakatani S et al (1995) Randomised trial of effects of interferon-alpha on incidence of hepatocellular carcinoma in chronic active hepatitis C with cirrhosis. *Lancet* 346:1051–1055
15. Yu ML, Lin SM, Chuang WL et al (2006) A sustained virological response to interferon or interferon/ribavirin reduces hepatocellular carcinoma and improves survival in chronic hepatitis C: a nationwide, multicentre study in Taiwan. *Antivir Ther* 11:985–994
16. Tanaka H, Tsukuma H, Kasahara A et al (2000) Effect of interferon therapy on the incidence of hepatocellular carcinoma and mortality of patients with chronic hepatitis C: a retrospective cohort study of 738 patients. *Int J Cancer* 87:741–749
17. Shiratori Y, Shiina S, Teratani T et al (2003) Interferon therapy after tumor ablation improves prognosis in patients with hepatocellular carcinoma associated with hepatitis C virus. *Ann Intern Med* 138:299–306
18. Kubo S, Nishiguchi S, Hirohashi K et al (2001) Effects of long-term postoperative interferon alpha therapy on intrahepatic recurrence after resection of hepatitis C virus-related hepatocellular carcinoma. A randomized, controlled trial. *Ann Intern Med* 134:963–967
19. Kubo S, Nishiguchi S, Hirohashi K et al (2002) Randomized clinical trial of long-term outcome after resection of hepatitis C virus-related hepatocellular carcinoma by postoperative interferon therapy. *Br J Surg* 89:418–422
20. Mazzaferro V, Romito R, Schiavo M et al (2006) Prevention of hepatocellular carcinoma recurrence with alpha-interferon after liver resection in HCV cirrhosis. *Hepatology* 44:1543–1554
21. Lin SM, Lin CJ, Hsu CW et al (2003) Prospective randomized controlled study of interferon-alpha in preventing hepatocellular carcinoma recurrence after medical ablation therapy for primary tumors. *Cancer (Phila)* 100:376–382
22. Lo CM, Liu CL, Chan SC et al (2007) A randomized, controlled trial of postoperative adjuvant interferon therapy after resection of hepatocellular carcinoma. *Ann Surg* 245:831–842
23. Ikeda K, Arase Y, Saitoh S et al (2000) Interferon beta prevents recurrence of hepatocellular carcinoma after complete resection or ablation of the primary tumor: a prospective randomized study of hepatitis C virus-related liver cancer. *Hepatology* 32:228–232
24. Sun HC, Tang ZY, Wang L et al (2006) Postoperative interferon alpha treatment postponed recurrence and improved overall survival in patients after curative resection of HBV-related hepatocellular carcinoma: a randomized clinical trial. *J Cancer Res Clin Oncol* 132:458–465
25. Sakaguchi Y, Kudo M, Fukunaga T et al (2005) Low-dose, long-term, intermittent interferon-alpha-2b therapy after radical treatment by radiofrequency ablation delays clinical recurrence in patients with hepatitis C virus-related hepatocellular carcinoma. *Intervirol* 48:64–70
26. Suou T, Mitsuda A, Koda M et al (2001) Interferon alpha inhibits intrahepatic recurrence in hepatocellular carcinoma with chronic hepatitis C: a pilot study. *Hepatol Res* 20:301–311
27. Hung CH, Lee CM, Wang JH et al (2005) Antiviral therapy after non-surgical tumor ablation in patients with hepatocellular carcinoma associated with hepatitis C virus. *J Gastroenterol Hepatol* 20:1553–1559
28. Jeong S, Aikata H, Katamura Y et al (2007) Low-dose intermittent interferon-alpha therapy for HCV-related liver cirrhosis after curative treatment of hepatocellular carcinoma. *World J Gastroenterol* 13:5188–5195
29. Kudo M, Sakaguchi Y, Chung H et al (2007) Long-term interferon maintenance therapy improves survival in patients with HCV-related hepatocellular carcinoma after curative radiofrequency ablation. A matched case-control study. *Oncology* 72(suppl 1):132–138
30. Someya T, Ikeda K, Saitoh S et al (2006) Interferon lowers tumor recurrence rate after surgical resection or ablation of hepatocellular carcinoma: a pilot study of patients with hepatitis B virus-related cirrhosis. *J Gastroenterol* 41:1206–1213
31. Cammà C, Di Bona D, Schepis F et al (2004) Effect of peg-interferon alfa-2a on liver histology in chronic hepatitis C: a meta-analysis of individual patient data. *Hepatology* 39:333–342
32. Lindsay KL, Trepo C, Heintges T et al (2001) A randomized, double-blind trial comparing pegylated interferon alfa-2b to

- interferon alfa-2b as initial treatment for chronic hepatitis C. *Hepatology* 34:395–403
33. Kumada H, Okanoue T, Onji M et al (2010) The Study Group for the Standardization of Treatment of Viral Hepatitis Including Cirrhosis, Ministry of Health, Labour, Welfare of Japan. Guidelines for the treatment of chronic hepatitis, cirrhosis due to hepatitis C virus infection for the fiscal year 2008 in Japan. *Hepatol Res* 40:8–13
 34. Parsons LS, Ovation Research Group (2001) Reducing bias in a propensity score matched-pair sample using greedy matching techniques. In: Proceedings of the Twenty-Sixth Annual SAS Users Group International Conference. SAS Institute Inc., Cary, pp 214–226
 35. Hisaka T, Yano H, Ogasawara S et al (2004) Interferon-alpha-Con1 suppresses proliferation of liver cancer cell lines in vitro and in vivo. *J Hepatol* 41:782–789
 36. Ogasawara S, Yano H, Momosaki S et al (2007) Growth inhibitory effects of IFN-beta on human liver cancer cells in vitro and in vivo. *J Interferon Cytokine Res* 27:507–516
 37. Nakaji M, Yano Y, Ninomiya T et al (2004) IFN-alpha prevents the growth of pre-neoplastic lesions and inhibits the development of hepatocellular carcinoma in the rat. *Carcinogenesis (Oxf)* 25:389–397
 38. Yano H, Ogasawara S, Momosaki S et al (2006) Growth inhibitory effects of pegylated IFN alpha-2b on human liver cancer cells in vitro and in vivo. *Liver Int* 26:964–975
 39. Miki A, Yano Y, Kato H et al (2008) Anti-tumor effect of pegylated interferon in the rat hepatocarcinogenesis model. *Int J Oncol* 32:603–608
 40. Chung RT, Andersen J, Volberding P et al (2004) Peginterferon Alfa-2a plus ribavirin versus interferon alfa-2a plus ribavirin for chronic hepatitis C in HIV-coinfected persons. *N Engl J Med* 351:451–459
 41. Carrat F, Bani-Sadr F, Pol S et al (2004) Pegylated interferon alfa-2b vs standard interferon alfa-2b, plus ribavirin, for chronic hepatitis C in HIV-infected patients: a randomized controlled trial. *JAMA* 292:2839–2848

ORIGINAL ARTICLES—LIVER, PANCREAS, AND BILIARY TRACT

Characteristics of Patients With Nonalcoholic Steatohepatitis Who Develop Hepatocellular Carcinoma

KOHICHIROH YASUI,* ETSUKO HASHIMOTO,[†] YASUJI KOMORIZONO,[§] KAZUHIKO KOIKE,^{||} SHIGEKI ARII,[¶] YASU HARU IMAI,[#] TOSHIHIDE SHIMA,** YOSHIHIRO KANBARA,** TOSHIJI SAIBARA,†† TAKAHIRO MORI,^{§§} SUMIO KAWATA,^{|||} HIROFUMI UTO,^{¶¶} SHIRO TAKAMI,^{###} YOSHIO SUMIDA,^{***} TOSHINARI TAKAMURA,^{†††} MIWA KAWANAKA,^{§§§} TAKESHI OKANOUE^{*,**} and the Japan NASH Study Group, Ministry of Health, Labour, and Welfare of Japan

*Department of Molecular Gastroenterology and Hepatology, Graduate School of Medical Science, Kyoto Prefectural University of Medicine, Kyoto; [†]Department of Internal Medicine and Gastroenterology, Tokyo Women's Medical University, Tokyo; [§]Department of Hepatology, Nanpuh Hospital, Kagoshima; ^{||}Department of Gastroenterology, Graduate School of Medicine, University of Tokyo, Tokyo; [¶]Department of Hepato-Biliary-Pancreatic Surgery, Tokyo Medical and Dental University, Tokyo; [#]Department of Internal Medicine, Ikeda Municipal Hospital, Ikeda; ^{**}Center of Gastroenterology and Hepatology, Saiseikai Suita Hospital, Suita; ^{††}Department of Gastroenterology and Hepatology, Kochi Medical School, Kochi; ^{§§}Department of Gastroenterology, Osaka Railway Hospital, Osaka; ^{|||}Department of Gastroenterology, Yamagata University School of Medicine, Yamagata; ^{¶¶}Digestive Disease and Life-style Related Disease Health Research, Human and Environmental Sciences, Kagoshima University Graduate School of Medical and Dental Sciences, Kagoshima; ^{###}Department of Gastroenterology, Otsu Municipal Hospital, Otsu; ^{***}Center for Digestive and Liver Diseases, Nara City Hospital, Nara; ^{†††}Department of Disease Control and Homeostasis, Kanazawa University, Graduate School of Medical Science, Kanazawa; and ^{§§§}Center of Liver Diseases, Kawasaki Hospital, Kawasaki Medical School, Okayama, Japan

This article has an accompanying continuing medical education activity on page e50. Learning Objectives—At the end of this activity, the learner should identify the clinical features of patients with nonalcoholic steatohepatitis who develop hepatocellular carcinoma and the role of hepatic fibrosis in the development of hepatocellular carcinoma.

See related article, Villanueva A et al, on page 1501 in *Gastroenterology*.

BACKGROUND & AIMS: Nonalcoholic steatohepatitis (NASH) can progress to hepatocellular carcinoma (HCC). We aimed to characterize the clinical features of NASH patients with HCC. **METHODS:** In a cross-sectional multicenter study in Japan, we examined 87 patients (median age, 72 years; 62% male) with histologically proven NASH who developed HCC. The clinical data were collected at the time HCC was diagnosed. **RESULTS:** Obesity (body mass index ≥ 25 kg/m²), diabetes, dyslipidemia, and hypertension were present in 54 (62%), 51 (59%), 24 (28%), and 47 (55%) patients, respectively. In nontumor liver tissues, the degree of fibrosis was stage 1 in 10 patients (11%), stage 2 in 15 (17%), stage 3 in 18 (21%), and stage 4 (ie, liver cirrhosis) in 44 (51%). The prevalence of cirrhosis was significantly lower among male patients (21 of 54, 39%) compared with female patients (23 of 33, 70%) ($P = .008$). **CONCLUSIONS:** Most patients with NASH who develop HCC are men; the patients have high rates of obesity, diabetes, and hypertension. Male patients appear to develop HCC at a less advanced stage of liver fibrosis than female patients.

Keywords: Liver Cancer; Incidence; Sex; Retrospective Study.

Hepatocellular carcinoma (HCC) is the fifth most common cancer worldwide and the third leading cause of cancer mortality.¹ HCC mostly occurs within an established back-

ground of chronic liver disease and cirrhosis. Although the risk factors for HCC, including infection with hepatitis B and C viruses as well as alcohol consumption, are well-defined, 5%–30% of patients with HCC lack a readily identifiable risk factor for their cancer. It has been suggested that a more severe form of nonalcoholic fatty liver disease (NAFLD), namely nonalcoholic steatohepatitis (NASH), might account for a substantial portion of cryptogenic cirrhosis and HCC cases.²

NAFLD is one of the most common causes of chronic liver disease in the world.^{3,4} NAFLD is associated with obesity, diabetes, dyslipidemia, and insulin resistance and is recognized as a hepatic manifestation of metabolic syndrome. The spectrum of NAFLD ranges from a relatively benign accumulation of lipid (simple steatosis) to progressive NASH associated with fibrosis, necrosis, and inflammation. Despite its common occurrence and potentially serious nature, relatively little is known about the natural history or prognostic significance of NAFLD. Although prospective studies on the natural history of NAFLD and NASH with a larger cohort are awaited, these

Abbreviations used in this paper: AFP, α -fetoprotein; ALT, alanine aminotransferase; AST, aspartate aminotransferase; BMI, body mass index; CT, computed tomography; DCP, des- γ -carboxy prothrombin; γ -GTP, γ -glutamyl transpeptidase; HCC, hepatocellular carcinoma; HDL, high-density lipoprotein; MRI, magnetic resonance imaging; NAFLD, nonalcoholic fatty liver disease; NASH, nonalcoholic steatohepatitis.

© 2011 by the AGA Institute
1542-3565/\$36.00
doi:10.1016/j.cgh.2011.01.023

studies might be limited by the long and asymptomatic clinical course of these diseases, by their high prevalence in the general population, and by the lack of serologic markers for NASH. The evidence suggesting that NASH can progress to HCC comes from (1) case reports and case series,⁵⁻⁸ (2) retrospective studies,⁹⁻¹² and (3) prospective studies.¹³⁻¹⁷ These studies generally examined limited numbers of cases and follow-ups; therefore, the incidence of HCC and risk factors for HCC in NASH patients remain unclear.

The Japan NASH Study Group (representative, Takeshi Okanoue)¹⁸ was established in 2008 by the Ministry of Health, Labour and Welfare of Japan to address unmet research needs in the area of liver diseases. As a part of this mandate, the study group conducted a cross-sectional multicenter study to characterize the clinical features of histologically proven NASH patients who developed HCC.

Methods

Patients

We retrospectively identified and reviewed 87 Japanese patients with NASH, who developed HCC between 1993 and 2010, at 15 hepatology centers that belong to the Japan NASH Study Group¹⁸ and their affiliated hospitals in Japan. The diagnosis of NASH was based on (1) the histologic features of steatohepatitis, (2) negligible alcohol consumption, and (3) exclusion of liver diseases of other etiology. To determine alcohol consumption as accurately as possible, we reviewed medical records in our institutions, and when patients had been transferred from other institutions, we also reviewed a summary of medical records from those institutions. According to the medical records, alcohol consumption was assessed on the basis of a detailed history that was obtained by physicians and by interviewing family members. Exclusion criteria included consumption of more than 20 g of alcohol per day, positivity for hepatitis B virus surface antigen, positivity for anti-hepatitis C virus antibody, the presence of other types of liver diseases (eg, primary biliary cirrhosis, autoimmune hepatitis, Wilson's disease, or hemochromatosis), previous treatment with drugs known to produce hepatic steatosis, and a history of gastrointestinal bypass surgery. The sections of nontumor liver tissues were reanalyzed by experienced hepatopathologists (T.O., E.H.) who were blinded to the laboratory parameters and clinical data. We excluded patients whose histologic diagnosis of NASH was not confirmed by central review and patients with insufficient or inconclusive information concerning alcohol consumption, body mass index (BMI), and laboratory data including fasting glucose and lipid.

Of the 87 patients, 14 patients had been previously diagnosed as NAFLD or NASH and had been followed at our institutions; 73 patients had been transferred from other institutions to our institutions for investigation and treatment of HCC. Most patients had been identified as having HCC during screening, which included ultrasound and/or computed tomography (CT) of the liver and alpha-fetoprotein (AFP) testing.

The diagnosis of HCC was based on liver histology and, in the absence of histology, on typical features of HCC as assessed by dynamic CT or magnetic resonance imaging (MRI) (ie, hypervascular with washout in the portal/venous phase).¹⁹ Of the 87 patients, 49 patients were diagnosed as HCC after hepatic resection, 21 patients were diagnosed after ultrasound-guided

tumor biopsy, and 17 patients were diagnosed by dynamic CT or MRI.

The Ethics Committees of each participating center approved this study. Informed consent was obtained from each patient in accordance with the Declaration of Helsinki.

Clinical Assessment and Laboratory Tests

The clinical and laboratory data were collected at the time HCC was diagnosed. BMI was calculated by using the following formula: weight in kilograms/(height in meters)². Obesity was defined as BMI ≥ 25 kg/m² according to the criteria of the Japan Society for the Study of Obesity.²⁰ Diabetes was defined as fasting plasma glucose concentration of ≥ 126 mg/dL or 2-hour plasma glucose concentration of ≥ 200 mg/dL during an oral glucose (75 g) tolerance test or by the use of insulin or oral hypoglycemic agents to control blood glucose.²¹ Hypertension was defined as systolic blood pressure ≥ 130 mm Hg or diastolic blood pressure ≥ 85 mm Hg or by the use of antihypertensive agents.²² Dyslipidemia was defined as serum concentrations of triglycerides ≥ 150 mg/dL or high-density lipoprotein (HDL) cholesterol < 40 mg/dL and < 50 mg/dL for men and women, respectively, or by the use of specific medication.²²

Venous blood samples were taken in the morning after 12-hour overnight fast. The laboratory evaluations included blood cell count and measurement of serum aspartate aminotransferase (AST), alanine aminotransferase (ALT), γ -glutamyl transpeptidase (γ -GTP), fasting plasma glucose, HbA1c, total cholesterol, HDL cholesterol, triglyceride, ferritin, hyaluronic acid, AFP, and des- γ -carboxy prothrombin (DCP). These parameters were measured by using standard clinical chemistry techniques.

Histopathologic Examination

Nontumor liver tissues were obtained from all 87 patients to diagnose the background liver tissue at the time HCC was diagnosed. In 49 patients who underwent hepatic resection for HCC, we examined nontumor liver tissues that were surgically resected. In 21 patients who underwent ultrasound-guided tumor biopsy, nontumor liver tissues far from HCC tumors were biopsied separately. In 17 patients who were diagnosed as HCC by dynamic CT or MRI and did not undergo either hepatic resection or tumor biopsy, only nontumor liver tissues far from HCC tumors were obtained by ultrasound-guided biopsy.

The specimens were fixed in formalin, embedded in paraffin, and stained with hematoxylin-eosin, with Masson trichrome, and by silver impregnation. NASH was defined as steatosis with lobular inflammation, hepatocellular ballooning, and Mallory's hyaline (Mallory's body) or fibrosis.²³⁻²⁵ The necroinflammatory grade and the degree of fibrosis were evaluated and scored according to the criteria proposed by Brunt et al.²⁶

Statistical Analysis

Results are presented as numbers with percentages in parentheses for qualitative data or as the medians and ranges (25th-75th percentiles) for quantitative data. Comparisons were made by using a χ^2 test for qualitative factors or a Mann-

Table 1. Patient Characteristics

Characteristic	Total (n = 87)	Male (n = 54)	Female (n = 33)	P value ^a
Age (y)	72 (69–75)	72 (69–75)	72 (68–75)	.52
BMI (kg/m^2)	26.0 (23.8–28.3)	26.0 (23.8–28.8)	26.2 (23.9–27.7)	.54
Obesity	54 (62%)	35 (65%)	19 (58%)	.50
Diabetes	51 (59%)	31 (57%)	20 (61%)	.77
Dyslipidemia	24 (28%)	13 (24%)	11 (33%)	.35
Hypertension	47 (54%)	22 (41%)	25 (76%)	.001
Platelet count ($\times 10^4/\mu L$)	13.9 (10.1–18.0)	14.5 (11.7–18.0)	10.9 (7.8–18.0)	.05
AST (IU/L)	47 (30–59)	46 (27–60)	47 (35–58)	.45
ALT (IU/L)	36 (26–55)	43 (26–69)	34 (26–42)	.11
γ -GTP (IU/L)	75 (40–115)	68 (36–177)	75 (40–115)	.90
Fasting glucose (mg/dL)	114 (99–145)	112 (99–144)	120 (97–152)	.59
HbA1c (%)	6.1 (5.4–7.1)	5.9 (5.4–7.0)	6.3 (5.2–7.1)	.78
Total cholesterol (mg/dL)	169 (147–202)	169 (147–202)	169 (147–202)	.62
HDL cholesterol (mg/dL)	50 (41–60)	45 (41–58)	55 (50–73)	.03
Triglyceride (mg/dL)	100 (76–138)	118 (80–147)	96 (74–116)	.06
Ferritin (ng/dL) ^b	197 (74–401)	273 (154–703)	98 (23–172)	.005
Hyaluronic acid (ng/mL) ^c	166 (67–241)	151 (69–244)	174 (61–332)	.85
AFP (ng/mL)	7.1 (5.0–18.0)	6.0 (4.0–14.7)	10.8 (5.9–18.0)	.02
DCP (mAU/mL)	66 (22–298)	48 (22–243)	81 (21–942)	.42
HCC tumor size (cm)	3.0 (2.0–4.0)	3.1 (2.2–4.5)	2.6 (1.9–4.0)	.18
Number of HCC tumors				.78
1	65 (75%)	39 (72%)	26 (79%)	
2 or 3	16 (18%)	11 (20%)	5 (15%)	
≥ 4	6 (7%)	4 (8%)	2 (6%)	
Background liver tissue				
Steatosis grade				.64
0: <5%	1 (1%)	1 (2%)	0 (0%)	
1: 5%–33%	60 (69%)	36 (67%)	24 (73%)	
2: 34%–66%	19 (22%)	11 (20%)	8 (24%)	
3: >66%	7 (8%)	6 (11%)	1 (3%)	
Necroinflammatory grade ^d				.22
1: mild	31 (35%)	22 (41%)	9 (27%)	
2: moderate	45 (52%)	26 (48%)	19 (58%)	
3: severe	11 (13%)	6 (11%)	5 (15%)	
Fibrosis stage ^d				.003
1	10 (11%)	10 (18%)	0 (0%)	
2	15 (17%)	10 (18%)	5 (15%)	
3	18 (21%)	13 (25%)	5 (15%)	
4	44 (51%)	21 (39%)	23 (70%)	

NOTE. Values are medians (25th–75th percentiles) or numbers (%). Where no other unit is specified, values refer to number of patients.

^a χ^2 test or Mann–Whitney *U* test.

^bMissing data for 27 patients.

^cMissing data for 29 patients.

^dAccording to reference 26.

Whitney *U* test on ranks for quantitative factors with non-equal variance. *P* values less than .05 from two-sided tests were considered to be significant. All statistical analyses were performed by using SPSS 15.0 software (SPSS Inc, Chicago, IL).

Results

The characteristics of the 87 NASH patients who developed HCC are summarized in Table 1. The median age was 72 years (25th percentile, 69; 75th percentile, 75); the mean age (standard deviation) was 71.2 (6.7) years. There were 54 male patients (62%) and 33 female patients (38%); the male:female ratio was 1.6:1. The median BMI was 26.0 kg/m^2 , and 54 patients (62%) were obese (BMI ≥ 25 kg/m^2). Diabetes, dyslipidemia, and hypertension were present in 51 (59%), 24 (28%), and 47 (55%) patients, respectively.

The diagnosis of NASH was proved by histologic examination of nontumor liver tissues at the time HCC was diagnosed. The degree of steatosis was grade 1 (5%–33%) in 60 patients (69%), grade 2 (34%–66%) in 19 (22%), and grade 3 (>66%) in 7 (8%). One patient who showed less than 5% steatosis was diagnosed as “burn-out” NASH, because a previous liver biopsy that was performed before development of HCC had demonstrated typical histologic features of NASH. The necroinflammatory grade was mild (grade 1) in 31 patients (35%), moderate (grade 2) in 45 (52%), and severe (grade 3) in 11 (13%). The degree of fibrosis was stage 1 in 10 patients (11%), stage 2 in 15 (17%), stage 3 in 18 (21%), and stage 4 (ie, liver cirrhosis) in 44 (51%).

The median diameter of HCC tumors was 3.0 cm (25th percentile, 2.0; 75th percentile, 4.0). A single HCC lesion was present in 65 of 87 patients (75%).

Data were stratified according to sex (Table 1). Compared with female patients, male patients had significantly less hypertension, lower HDL cholesterol and AFP, higher ferritin, and a less advanced stage of fibrosis. The prevalence of cirrhosis was significantly lower in male patients (21 of 54, 39%) than in female patients (23 of 33, 70%) ($P = .008$).

Discussion

In this cross-sectional multicenter study in Japan, we showed the clinical features of a relatively large number ($n = 87$) of NASH patients with HCC. The male:female ratio was 1.6:1. Men have higher HCC rates than women in almost all populations, with male:female ratios usually averaging between 2:1 and 4:1.² In the latest nationwide survey of HCC in Japan,²⁷ this ratio was 2.5:1. The reasons underlying higher rates of HCC in men might relate to sex-specific differences in exposure to risk factors. Men are more likely to be infected with hepatitis B and C viruses, consume alcohol, smoke cigarettes, and have increased iron stores.² Moreover, androgens are considered to influence the development of HCC. With regard to the male:female ratio of HCC associated with NASH, a male:female ratio of 1.3:1 was reported in a summary of 16 published cases of HCC associated with NASH.²⁸ Ratios of 2.8:1 and 0.67:1 were reported in 2 retrospective studies of HCC arising from cryptogenic cirrhosis in Italy ($n = 44$)¹⁰ and the United States ($n = 30$),⁹ respectively, and a ratio of 1.6:1 was reported for 36 cases of NASH-associated HCC from a single center in Japan.¹⁵ Overall, NASH patients with HCC are more often men. However, these male:female ratios might be lower than the ratios for HCC of other etiologies, including viral hepatitis and alcohol consumption.

Although it is well-known that male gender is a risk factor for HCC in patients infected with hepatitis B and C viruses,² it remains unclear whether male gender is a factor associated with the development of HCC in NASH patients. It is now suspected that there is an even distribution of NASH among men and women.²⁹ In another study by our group,³⁰ the male:female ratio was 0.85:1 in 342 NASH patients without cirrhosis and HCC. The male:female ratio (1.6:1) of NASH patients with HCC in the present study is higher than this ratio. In agreement with our observations, a case-control study showed that the male:female ratio was 1.6:1 in 34 NASH patients with HCC, whereas the ratio was 0.69:1 in 348 NASH patients without HCC.¹⁵ A recent prospective study indicated that older age and alcohol consumption were independent risk factors for the development of HCC in patients with NASH-cirrhosis and that male gender tended to be associated with the development of HCC, although this trend did not reach statistical significance.¹⁷

The median age of our patients was 72 years. There was no significant difference in age between men and women. Although the global age distribution of HCC varies by geographic region, sex, and etiology, in almost all areas the peak female age group in HCC patients is 5 years older than in male HCC patients.² In a nationwide survey of HCC in Japan,²⁷ the mean ages were 65.5 years for men and 69.4 years for women. The male patients in the present study are slightly older than the mean ages reported in these previous studies.

Consistent with the literature,⁹⁻¹² more than half of our patients displayed obesity, diabetes, and hypertension. Obesity constitutes a significant risk factor for cancer mortality in

general and is an increasingly recognized risk factor for HCC in particular.^{31,32} In the present study, body weight was measured at the time HCC was diagnosed. Because advanced HCC might cause weight loss, it is likely that our patients were obese before the development of HCC. Diabetes has also been proposed as a risk factor for HCC.² Thus, HCC shares 2 major risk factors, obesity and diabetes, with NASH.

Once cirrhosis and HCC are established, it is difficult to identify pathologic features of NASH. As NASH progresses to cirrhosis, steatosis tends to disappear, so-called burn-out NASH.⁵ As expected, the grade of steatosis was mild in most of our cases. It was possible to diagnose 1 case without steatosis as burn-out NASH, because a previous liver biopsy specimen (liver biopsy was performed 25 years prior) was preserved and available. It is likely that many cases of NASH-associated HCC might have been missed because of loss of the telltale sign of steatosis.

Most HCC arises on a background of cirrhosis. It is less clear whether cirrhosis is a necessary predisposition for the development of HCC in patients with NASH. Case reports of HCC arising from NAFLD and NASH patients without fibrosis or cirrhosis have been accumulating.³³⁻³⁶ Cirrhosis (fibrosis stage 4) was present in 51% of cases, and advanced stages of fibrosis (stage 3 or 4) were found in 72% of cases in the present study. Indeed, cirrhosis or advanced fibrosis appeared to be the predominant risk factors for HCC development. However, in the remaining 28% of cases, HCC developed in patients with less fibrosis (stage 1 or 2). Interestingly, male patients developed HCC at a less advanced stage of fibrosis than female patients, and the prevalence of cirrhosis was significantly lower in men (39%) than in women (70%). Although the reason for the sex differences is unclear, these findings indicate that screening for HCC is needed not only in NASH patients with advanced fibrosis but also in those with less fibrosis, particularly if they are men. Further studies are needed to confirm this potentially important observation. Paradis et al³⁷ reported that in patients whose only risk factors for chronic liver disease are features of metabolic syndrome, HCC usually occurs in the absence of significant liver fibrosis. In addition, they found that some of these HCCs developed on preexisting liver cell adenomas. However, no preexisting adenomas were observed in the present cases.

Compared with female patients, male patients had significantly higher serum ferritin value. The normal value for ferritin varies according to the age and gender of the individual. Adult men have serum ferritin values averaging approximately 100 ng/mL (range, 75-250), whereas adult women have levels averaging approximately 30 ng/mL (range, 20-75).³⁸ Thus, normal men have higher ferritin levels than women. Elevation of ferritin levels is associated with NASH.³⁹ Because we excluded patients with alcohol consumption as rigorously as possible, we believe that alcohol consumption did not contribute to the elevation of ferritin levels in our patients.

The median diameter of the HCCs in the present study was 3.0 cm, which is equal to or smaller than the size of previously reported HCCs.^{9,10,12,28,37} This is probably because most of our patients had been identified as having HCC during screening. A single HCC lesion was present in 75% of patients. For early detection of NASH-associated HCC, vigilant screening is important,⁹ and the development of serologic markers for NASH is necessary.

The mechanisms of carcinogenesis in NASH remain to be elucidated. Possible mechanisms include hyperinsulinemia

caused by insulin resistance in NASH, increased levels of insulin-like growth factor that promotes tumor growth, increased susceptibility of the steatotic liver to lipid peroxidation, production of reactive oxygen species and subsequent DNA mutations, disordered energy and hormonal regulation in obesity, and aberrations in regenerative processes occurring in cirrhosis.²⁵

Certain limitations should be considered in the interpretation of our findings. First, the cross-sectional study design hinders the ability to draw inferences regarding the causality of NASH in HCC. Second, the study did not include a control group of HCC patients with other liver diseases. Third, there might be a bias in patient selection, because patients were retrospectively identified as having NASH-associated HCC. Finally, although our patients were negative for hepatitis B virus surface antigen, it is still possible that occult hepatitis B virus infection might be associated with the development of HCC in some of our cases.

In summary, we showed the clinical features of NASH patients with HCC. NASH patients with HCC were more often men and frequently displayed obesity, diabetes, and hypertension. Our results suggest that male patients might develop HCC at a less advanced stage of fibrosis than female patients. Further prospective studies with a longer follow-up time and larger cohorts are needed to determine the causal association of NASH with HCC and to identify risk factors for the development of HCC in NASH patients.

References

- Parkin DM. Global cancer statistics in the year 2000. *Lancet Oncol* 2001;2:533–543.
- El-Serag HB, Rudolph KL. Hepatocellular carcinoma: epidemiology and molecular carcinogenesis. *Gastroenterology* 2007;132:2557–2576.
- Farell GC, Larter CZ. Nonalcoholic fatty liver disease: from steatosis to cirrhosis. *Hepatology* 2006;43:S99–S112.
- Angulo P. Nonalcoholic fatty liver disease. *N Engl J Med* 2002;346:1221–1231.
- Powell EE, Cooksley WG, Hanson R, et al. The natural history of nonalcoholic steatohepatitis: a follow-up study of forty-two patients for up to 21 years. *Hepatology* 1990;11:74–80.
- Cotrim HP, Parana R, Braga E, et al. Nonalcoholic steatohepatitis and hepatocellular carcinoma: natural history? *Am J Gastroenterol* 2000;95:3018–3019.
- Zen Y, Katayanagi T, Tsuneyama K, et al. Hepatocellular carcinoma arising in non-alcoholic steatohepatitis. *Pathol Int* 2001;51:127–131.
- Shimada M, Hashimoto E, Taniai M, et al. Hepatocellular carcinoma in patients with non-alcoholic steatohepatitis. *J Hepatol* 2002;37:154–160.
- Marrero JA, Fontana RJ, Su GL, et al. NAFLD may be a common underlying liver disease in patients with hepatocellular carcinoma in the United States. *Hepatology* 2002;36:1349–1354.
- Bugianesi E, Leone N, Vanni E, et al. Expanding the natural history of nonalcoholic steatohepatitis: from cryptogenic cirrhosis to hepatocellular carcinoma. *Gastroenterology* 2002;123:134–140.
- Ratzliff V, Bonyhay L, Di Martino V, et al. Survival, liver failure, and hepatocellular carcinoma in obesity-related cryptogenic cirrhosis. *Hepatology* 2002;35:1485–1493.
- Regimbeau JM, Colombat M, Mognol P, et al. Obesity and diabetes as a risk factor for hepatocellular carcinoma. *Liver Transpl* 2004;10:S69–S73.
- Adams LA, Lymp JF, St Sauver J, et al. The natural history of nonalcoholic fatty liver disease: a population-based cohort study. *Gastroenterology* 2005;129:113–121.
- Sanyal AJ, Banas C, Sargeant C, et al. Similarities and differences in outcomes of cirrhosis due to nonalcoholic steatohepatitis and hepatitis C. *Hepatology* 2006;43:682–689.
- Hashimoto E, Yatsuji S, Tobari M, et al. Hepatocellular carcinoma in patients with nonalcoholic steatohepatitis. *J Gastroenterol* 2009;44:89–95.
- Yatsuji S, Hashimoto E, Tobari M, et al. Clinical features and outcomes of cirrhosis due to non-alcoholic steatohepatitis compared with cirrhosis caused by chronic hepatitis C. *J Gastroenterol Hepatol* 2009;24:248–254.
- Ascha MS, Hanouneh IA, Lopez R, et al. The incidence and risk factors of hepatocellular carcinoma in patients with nonalcoholic steatohepatitis. *Hepatology* 2010;51:1972–1978.
- Okanoue T, Umemura A, Yasui K, et al. Nonalcoholic fatty liver disease and nonalcoholic steatohepatitis in Japan. *J Gastroenterol Hepatol* 2011;26(Suppl 1):153–162.
- Bruix J, Sherman M, Practice Guidelines Committee, American Association for the Study of Liver Diseases. Management of hepatocellular carcinoma. *Hepatology* 2005;42:1208–1236.
- Japan Society for the Study of Obesity. New criteria of obesity (in Japanese). *J Jpn Soc Study Obes* 2000;6:18–28.
- Kuzuya T, Nakagawa S, Satoh J, et al. Report of the Committee on the classification and diagnostic criteria of diabetes mellitus. *Diabetes Res Clin Pract* 2002;55:65–85.
- Expert Panel on Detection, Evaluation, and Treatment of High Blood Cholesterol in Adults. Executive summary of the third report of the National Cholesterol Education Program (NCEP) Expert Panel on Detection, Evaluation, and Treatment of High Blood Cholesterol in Adults (Adult Treatment Panel III). *JAMA* 2001;285:2486–2497.
- Matteoni CA, Younossi ZM, Gramlich T, et al. Nonalcoholic fatty liver disease: a spectrum of clinical and pathological severity. *Gastroenterology* 1999;116:1413–1419.
- Kleiner DE, Brunt EM, Van Natta M, et al. Design and validation of a histological scoring system for nonalcoholic fatty liver disease. *Hepatology* 2005;41:1313–1321.
- Brunt EM. Non-alcoholic fatty liver disease. In: Burt AD, Portmann BC, Ferrell LD, eds. *MacSween's pathology of the liver*. 5th ed. London: Churchill Livingstone, 2006:367–397.
- Brunt EM, Janney CG, Di Bisceglie AM, et al. Non-alcoholic steatohepatitis: a proposal for grading and staging the histological lesions. *Am J Gastroenterol* 1999;94:2467–2474.
- Ikai I, Arii S, Okazaki M, et al. Report of the 17th Nationwide Follow-up Survey of Primary Liver Cancer in Japan. *Hepatol Res* 2007;37:676–691.
- Bugianesi E. Non-alcoholic steatohepatitis and cancer. *Clin Liver Dis* 2007;11:191–207.
- Neuschwander-Tetri BA, Caldwell SH. Nonalcoholic steatohepatitis: summary of an AASLD single topic conference. *Hepatology* 2003;37:1202–1219.
- Sumida Y, Yoneda M, Hyogo H, et al. A simple clinical scoring system using ferritin, fasting insulin and type IV collagen 7S for predicting steatohepatitis in nonalcoholic fatty liver disease. *J Gastroenterol* 2011;46:257–268.
- Calle EE, Rodriguez C, Walker-Thurmond K, et al. Overweight, obesity, and mortality from cancer in a prospectively studied cohort of U.S. adults. *N Engl J Med* 2003;348:1625–1638.
- Caldwell S, Park SH. The epidemiology of hepatocellular cancer: from the perspectives of public health problem to tumor biology. *J Gastroenterol* 2009;44:96–101.
- Bullock RE, Zaitoun AM, Aithal GP, et al. Association of non-alcoholic steatohepatitis without significant fibrosis with hepatocellular carcinoma. *J Hepatol* 2004;41:685–686.
- Ichikawa T, Yanagi K, Motoyoshi Y, et al. Two cases of non-alcoholic steatohepatitis with development of hepatocellular carcinoma without cirrhosis. *J Gastroenterol Hepatol* 2006;21:1865–1866.
- Guzman G, Brunt EM, Petrovic LM, et al. Does nonalcoholic fatty liver disease predispose patients to hepatocellular carcinoma in the absence of cirrhosis? *Arch Pathol Lab Med* 2008;132:1761–1766.

36. Kawada N, Imanaka K, Kawaguchi T, et al. Hepatocellular carcinoma arising from non-cirrhotic nonalcoholic steatohepatitis. *J Gastroenterol* 2009;44:1190–1194.
37. Paradis V, Zalinski S, Chelbi E, et al. Hepatocellular carcinomas in patients with metabolic syndrome often develop without significant liver fibrosis: a pathological analysis. *Hepatology* 2009;49:851–859.
38. Adamson JW. Hematopoietic disorders. In: Fauci AS, Braunwald E, Kasper DL, et al, eds. *Harrison's principles of internal medicine*. 17th ed. New York: McGraw-Hill Companies, 2008:628–634.
39. Bonkovsky HL, Jawaid Q, Tortorelli K, et al. Non-alcoholic steatohepatitis and iron: increased prevalence of mutations of the HFE gene in non-alcoholic steatohepatitis. *J Hepatol* 1999;31:421–429.

Reprint requests

Address requests for reprints to: Takeshi Okanoue, MD, PhD, Director, Center of Gastroenterology and Hepatology, Saiseikai Suita Hospital, 1-2 Kawazono-cho, Suita 5640013, Japan. e-mail: okanoue@suita.saiseikai.or.jp; fax: +81-6-6382-1524.

Conflicts of interest

The authors disclose no conflicts.

Funding

This work was supported by a grant from the Ministry of Health, Labour and Welfare of Japan (H20-hepatitis-008 to Takeshi Okanoue).

Hypervascular hepatocellular carcinomas: detection with gadoxetate disodium-enhanced MR imaging and multiphase multidetector CT

Hiromitsu Onishi · Tonsok Kim · Yasuharu Imai · Masatoshi Hori · Hiroaki Nagano · Yasuhiro Nakaya · Takahiro Tsuboyama · Atsushi Nakamoto · Mitsuaki Tatsumi · Seishi Kumano · Masahiro Okada · Manabu Takamura · Kenichi Wakasa · Noriyuki Tomiyama · Takamichi Murakami

Received: 4 July 2011 / Revised: 29 September 2011 / Accepted: 15 October 2011
© European Society of Radiology 2011

Abstract

Objectives To retrospectively compare the accuracy of detection of hypervascular hepatocellular carcinoma (HCC) by multiphase multidetector CT and by gadoxetate disodium-enhanced MR imaging.

Methods After ethical approval, we analysed a total of 73 hypervascular HCC lesions from 31 patients suspected of having HCC, who underwent both gadoxetate disodium-enhanced MR imaging and multiphase multidetector CT. Five blinded observers independently reviewed CT images, as well as dynamic MR images alone and combined with hepatobiliary phase MR images. Diagnostic accuracy (Az values), sensitivities and positive predictive values were compared by using the Scheffe post hoc test.

Results The mean Az value for dynamic and hepatobiliary phase MR combined (0.81) or dynamic MR images alone (0.78) was significantly higher than that for CT images

(0.67, $P < 0.001$, 0.005, respectively). The mean sensitivity of the combined MR images (0.67) was significantly higher than that of dynamic MR alone (0.52, $P < 0.05$) or CT images (0.44, $P < 0.05$). The mean positive predictive values were 0.96, 0.95 and 0.94, for CT, dynamic MR alone and combined MR images, respectively.

Conclusions Compared with multiphase multidetector CT, gadoxetate disodium-enhanced MR imaging combining dynamic and hepatobiliary phase images results in significantly improved sensitivity and diagnostic accuracy for detection of hypervascular HCC.

Key Points

- Gadoxetate disodium is a new liver-specific MR imaging contrast agent. Gadoxetate disodium-enhanced MRI helps the assessment of patients with liver disease.
- It showed high diagnostic accuracy for the detection of hepatocellular carcinoma.

H. Onishi (✉) · T. Kim · M. Hori · Y. Nakaya · T. Tsuboyama · A. Nakamoto · M. Tatsumi · N. Tomiyama
Department of Radiology,
Osaka University Graduate School of Medicine,
2-2, Yamadaoka,
Suita, Osaka 565-0871, Japan
e-mail: h-onishi@iris.dti.ne.jp

Y. Imai
Department of Gastroenterology, Ikeda Municipal Hospital,
3-1-18, Johnan,
Ikeda, Osaka 563-8510, Japan

H. Nagano
Department of Surgery,
Osaka University Graduate School of Medicine,
2-2, Yamadaoka,
Suita, Osaka 565-0871, Japan

S. Kumano · M. Okada · T. Murakami
Department of Radiology, Kinki University School of Medicine,
377-2, Ohno-higashi,
Osakasayama, Osaka 589-8511, Japan

M. Takamura
Department of Radiology, Ikeda Municipal Hospital,
3-1-18, Johnan,
Ikeda, Osaka 563-8510, Japan

K. Wakasa
Department of Diagnostic Pathology,
Osaka City University Graduate School of Medicine,
1-4-3, Asahimachi, Abeno,
Osaka, Osaka 545-8585, Japan

Keywords Hepatocellular carcinoma · Magnetic resonance imaging · Computed tomography · Comparative study · Gadoxetate disodium

Introduction

Along with biopsy, diagnostic imaging such as multiphase computed tomography (CT) or magnetic resonance (MR) imaging is reliably used for the assessment of hepatocellular carcinoma (HCC) [1–5]. According to the diagnostic algorithm suggested by the American Association for the Study of Liver Diseases (AASLD), a hepatic mass larger than 1 cm in diameter in a cirrhotic liver that demonstrates a typical vascular pattern (arterial hypervascularity and “washout” in the equilibrium phase) on CT or MR imaging can be diagnosed as HCC without biopsy [1, 2]. Evaluation of lesion vascularity (i.e. hypervascular or hypovascular) as well as detection of the focal lesion are thus essential elements of diagnosis of HCC through imaging.

Gadoxetate disodium (Primovist) is a liver-specific MR imaging contrast agent taken up by hepatocytes [6–12] and facilitates accurate detection of focal liver lesions on MR images during the hepatobiliary phase [13–21]. Several studies have compared gadoxetate disodium-enhanced MR imaging with multiphase multidetector CT for the detection of HCC [22–24]. To the best of our knowledge, however, the literature contains no comparative study of the diagnostic accuracy for the detection of hypervascular HCC which is also based on careful evaluation of tumour vascularity. Use of gadoxetate disodium produces not only liver-specific hepatobiliary but also dynamic MR images, which makes it possible to evaluate tumour vascularity [22–30]. However, since the amount of gadolinium in gadoxetate disodium medium (0.025 mmol/kg) is smaller than that in extracellular gadolinium chelates medium (0.1 mmol/kg) at the recommended dosage, dynamic MR imaging using gadoxetate disodium could impair tumour enhancement in the arterial dominant phase [31] and compromise characterisation of the lesions based on vascularity.

The purpose of our study was to retrospectively compare the accuracy for detection of hypervascular HCC by means of multiphase multidetector CT and gadoxetate disodium-enhanced MR imaging.

Materials and methods

This retrospective study was implemented at three institutions (Osaka University Hospital, Kinki University Hospital, and Ikeda Municipal Hospital) and approved, with waiver of informed consent, by the ethics committee of each institution.

Patient population

Ninety-seven consecutive patients with chronic liver disease and suspected of having HCC, who underwent both multiphase multidetector CT and gadoxetate disodium-enhanced MR imaging within a 6-week period between March and December, 2008, were eligible for the study. However, 66 (68%) of these patients were excluded from the study population because no angio-CT including double-phase CT during hepatic arteriography (CTHA) nor CT during arterial portography (CTAP) was performed ($n=61$), or because of inadequate MR examination ($n=5$). The remaining 31 patients (28 men and 3 women; mean age, 70.2 years; range, 52–82 years) constituted the study population (Fig. 1). Four of them had hepatitis B, 21 had hepatitis C, four had alcohol-related hepatitis and one had nonalcoholic steatohepatitis. Total bilirubin values of these patients ranged from 0.4 to 2.2 mg/dL (mean, 1.0 mg/dL). Twenty-three patients were classified as Child-Pugh A, and the remaining eight patients were classified as Child-Pugh B.

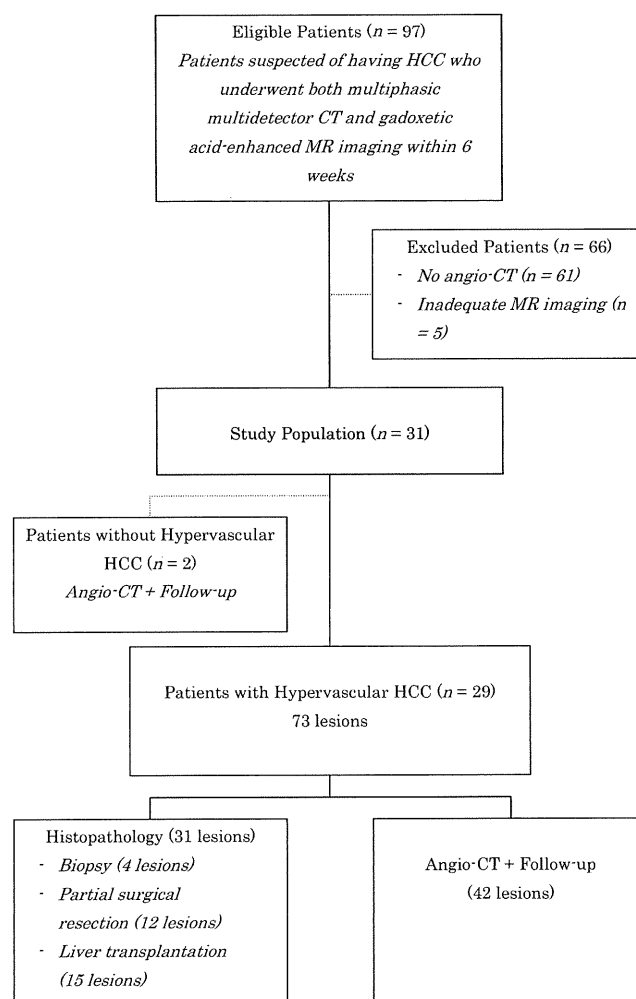


Fig. 1 Flowchart of patient enrollment and proof of tumour burden

Twenty-five of the patients underwent multidetector CT before MR imaging, and the mean interval between CT and MR imaging was 19 days.

Proof of tumour burden

Of the 31 patients evaluated, 29 had a total of 73 confirmed hypervascular HCC nodules. The nodules ranged from 0.3 to 14 cm in diameter (mean, 1.8 cm). While 31 HCC nodules were diagnosed histologically (partial surgical resection, $n=12$; biopsy, $n=4$; liver transplantation, $n=15$), the remaining 42 hypervascular HCCs were diagnosed clinically on the basis of tumour markers, double-phase CTHA and CTAP [32], follow-up CT and/or MR imaging (mean follow-up, 19 months; range 4–26 months). Whether the HCC nodules were of the arterial hypervascular or arterial hypovascular type was determined on the basis of the CTHA findings. Two patients had no hypervascular HCCs.

Multiphasic multidetector CT

Multiphasic CT was performed by using an 8-channel CT ($n=9$) (LightSpeed Ultra; GE Healthcare, Milwaukee, WI) or 64-channel CT ($n=22$) (LightSpeed VCT; GE Healthcare). The X-ray tube voltage was 120 kVp and the tube current was modulated automatically according to the patient's body size by means of an automatic tube current modulation technique (3D AutomA; GE Healthcare). The section thickness was 5 mm. All patients were given 2.0 mL (600 mg of iodine) per kilogram of body weight, with a maximum dose of 150 mL per patient, and 300 mgI/mL of the nonionic contrast medium. The warmed contrast medium was administered intravenously with a mechanical power injector at 3–5 mL/s with a fixed injection duration of 30 s through a 20-gauge catheter inserted into an arm vein. Multiphasic CT was performed immediately before contrast-medium administration and during the hepatic arterial dominant, portal venous dominant and equilibrium phases 30–45, 65–80, and 190–205 s, respectively, after the start of the contrast material injection [22–24, 33–35]. To determine

the acquisition delay for hepatic arterial dominant phase imaging, a semiautomatic bolus-tracking technique was used (SmartPrep; GE Healthcare). Arterial dominant phase acquisition was started 22 s after the trigger threshold (50HU elevation) was reached at the suprarenal abdominal aorta.

MR imaging

MR imaging was performed with a 1.5-T system ($n=23$) (Signa Excite HD 1.5T; GE Healthcare, or Intera; Philips Medical Systems, Eindhoven, The Netherlands) or 3.0-T system ($n=8$) (Signa HD 3.0T; GE Healthcare) with body-array coils. For the contrast enhancement, 0.1 mL/kg (0.025 mmol/kg) of gadoxetate disodium (Primovist; Bayer-Schering Pharma AG, Berlin, Germany) diluted with saline to 10 mL (e.g. a patient with a body weight of 60 kg received 6 mL of gadoxetate disodium medium diluted with 4 mL of saline) was administered intravenously with a mechanical power injector at 1 mL/s with a fixed injection duration of 10 s through a 22-gauge catheter inserted into an arm vein, followed by a 30-mL saline flush at 1 mL/s. However, the maximum applied dose of gadoxetate disodium was 10 mL (2.5 mmol).

For MR imaging, in-phase and out-of-phase T1-weighted images, T2-weighted images, gadoxetate disodium-enhanced dynamic images (precontrast, arterial, and portal venous dominant phase), and hepatobiliary phase images (20 min after the injection) were acquired. Acquisition parameters are listed in Table 1. Gadoxetate disodium-enhanced dynamic imaging was performed with three-dimensional gradient-echo sequences (LAVA; GE Healthcare or THRIVE; Philips Medical Systems), and performed immediately before contrast-medium administration and during the hepatic arterial dominant and portal venous dominant phases 25–40 and 70 s, respectively, after the start of the contrast material injection. To determine the acquisition delay for hepatic arterial dominant phase imaging, the bolus tracking technique was used. Arterial dominant phase acquisition was started 15 s after the trigger point was reached at the suprarenal abdominal aorta.

Table 1 MR imaging sequences and parameters

Acquisition	Sequence	TR (ms)	TE (ms)	ETL	Flip angle (degrees)	FOV (mm)	Matrix	Thickness (mm)	Fat suppression
T1 in-phase	2D GRE	175–220	4.4 (5.8)	–	12	340×340	192×320	5	Not used
T1 out-of-phase	2D GRE	175–220	2.2 (2.6)	–	12	340×340	192×320	5	Not used
T2-w.i.	2D FSE	6666–10000	89–93	8	90	340×340	160×512	5	Used
Dynamic & HB	3D GRE (LAVA or THRIVE)	4.5–4.8	2.2–2.3	–	12	340×340	192×320	4	Used

Numbers in parentheses show parameters at 3.0T. TR repetition time, TE echo time, ETL echo train length, FOV field of view, w.i. weighted image, 3D three-dimensional, GRE gradient echo, 2D two-dimensional, FSE fast spin echo, HB hepatobiliary phase image, LAVA liver acquisition with volume acceleration, THRIVE T1 high-resolution isotropic volume excitation

Table 2 Az values for the detection of hypervascular HCC

	Reader 1	Reader 2	Reader 3	Reader 4	Reader 5	Mean
All lesions (<i>n</i> =73)						
Multiphase CT	0.68	0.68	0.69	0.62	0.70	0.67*†
Dynamic MR imaging	0.78	0.73	0.80	0.78	0.83	0.78*
Combined dynamic and hepatobiliary phase MR imaging	0.84	0.74	0.80	0.82	0.86	0.81†
Lesions <1.0 cm (<i>n</i> =28)						
Multiphase CT	0.55	0.60	0.50	0.46	0.57	0.53‡§
Dynamic MR imaging	0.78	0.72	0.82	0.79	0.82	0.79‡
Combined dynamic and hepatobiliary phase MR imaging	0.79	0.77	0.80	0.78	0.84	0.80§
Lesions 1.0–2.0 cm (<i>n</i> =32)						
Multiphase CT	0.89	0.89	0.86	0.83	0.88	0.87
Dynamic MR imaging	0.86	0.72	0.80	0.79	0.90	0.81
Combined dynamic and hepatobiliary phase MR imaging	0.93	0.79	0.84	0.86	DD	0.85
Lesions >2.0 cm (<i>n</i> =13)						
Multiphase CT	DD	DD	DD	DD	DD	N/A
Dynamic MR imaging	DD	DD	DD	DD	DD	N/A
Combined dynamic and hepatobiliary phase MR imaging	DD	DD	0.99	DD	DD	0.99

DD degenerate data. *CT vs. dynamic MR: $P<0.01$, †CT vs. combined MR: $P<0.001$, ‡CT vs. dynamic MR: $P<0.001$, §CT vs. combined MR: $P<0.001$, and there were no statistically significant differences at other pairings among the three imaging techniques. (Scheffe post-hoc multiple comparison)

Qualitative image analysis

For each patient, multiphase multidetector CT images, gadopentate disodium-enhanced dynamic MR images with T1- and T2-weighted images, and all MR images including

hepatobiliary phase images were evaluated independently and blindly by five radiologists (readers 1, 2, 3, 4, and 5, with 19, 16, 8, 6, and 6 years experience, respectively, in gastrointestinal and hepatobiliary imaging). The images were read on a commercially available workstation. During one session,

Table 3 Sensitivity in the detection of hypervascular HCC

	Reader 1	Reader 2	Reader 3	Reader 4	Reader 5	Mean
All lesions (<i>n</i> =73)						
Multiphase CT	0.37 (27)	0.40 (29)	0.53 (39)	0.36 (26)	0.56 (41)	0.44*
Dynamic MR imaging	0.41 (30)	0.53 (39)	0.60 (44)	0.45 (33)	0.59 (43)	0.52†
Combined dynamic and hepatobiliary phase MR imaging	0.67 (49)	0.63 (46)	0.63 (46)	0.71 (52)	0.73 (53)	0.67*†
Lesions <1.0 cm (<i>n</i> =28)						
Multiphase CT	0.07 (2)	0.07 (2)	0.18 (5)	0.00 (0)	0.21 (6)	0.11‡
Dynamic MR imaging	0.11 (3)	0.29 (8)	0.36 (10)	0.14 (4)	0.29 (8)	0.24§
Combined dynamic and hepatobiliary phase MR imaging	0.46 (13)	0.43 (12)	0.43 (12)	0.57 (16)	0.50 (14)	0.48‡§
Lesions 1.0–2.0 cm (<i>n</i> =32)						
Multiphase CT	0.44 (14)	0.50 (16)	0.72 (23)	0.47 (15)	0.75 (24)	0.58
Dynamic MR imaging	0.47 (15)	0.59 (19)	0.69 (22)	0.56 (18)	0.72 (23)	0.61
Combined dynamic and hepatobiliary phase MR imaging	0.72 (23)	0.69 (22)	0.69 (22)	0.81 (26)	0.84 (27)	0.75
Lesions >2.0 cm (<i>n</i> =13)						
Multiphase CT	0.85 (11)	0.85 (11)	0.85 (11)	0.85 (11)	0.85 (11)	0.85
Dynamic MR imaging	0.85 (11)	0.92 (12)	0.92 (12)	0.69 (9)	0.92 (12)	0.86
Combined dynamic and hepatobiliary phase MR imaging	1.00 (13)	0.92 (12)	0.92 (12)	0.77 (10)	0.92 (12)	0.91

Numbers in parentheses are actual numbers of lesions. * CT vs. combined MR: $P<0.01$, †dynamic MR vs. combined MR: $P<0.05$, ‡CT vs. combined MR: $P<0.001$, §dynamic MR vs. combined MR: $P<0.01$, and there were no statistically significant differences at other pairings among the three imaging techniques. (Scheffe post-hoc multiple comparison)

image sets consisting of a mixture of MR images of half of the patients and CT images of the other half were presented in random order. During the other session, the remaining image sets were presented in random order. To minimise recall bias, each reading session was separated by at least 4 weeks.

Before the first reading session, the following criteria for diagnosing hypervascular HCC were provided to the readers: a) hyperenhancement during the hepatic arterial dominant phase; b) hypoattenuation or hypointensity compared with the surrounding liver during the portal venous or equilibrium phases (i.e. washout); c) hypointensity during the hepatobiliary phase; d) inhomogeneous isointensity or hyperintensity during the hepatobiliary phase [28, 33, 36, 37] and e) fat component in the nodule (lower attenuation than water on unenhanced CT images or signal reduction in the out-of-phase T1-weighted MR images in comparison with in-phase images). Hypervascular HCC was unequivocally diagnosed if a lesion fulfilled criterion (a) and any one of the other criteria (b–e). In addition, criteria for suspected but non-conclusive diagnosis of hypervascular HCC included f) mild hyperintensity on T2-weighted MR images with early enhancement or g) nodular arterial enhancement without

washout. Hemangioma was differentiated from HCC on the basis of the following image findings: a) a globular enhancement pattern during the hepatic arterial dominant phase, b) prolonged enhancement during the portal venous or equilibrium phases on CT images and c) significant hyperintensity on T2-weighted MR images.

Each reader classified all detected lesions according to the following four-point confidence score scale: 1- probably no mass lesion present; 2- indefinite presence of lesion; 3- lesion probably present; and 4- definite presence of a lesion; with confidence scores of 3 and 4 representing a positive diagnosis of liver mass lesion. For evaluation of MR images, the readers, after reading the dynamic MR images with T1- and T2-weighted images and recording the decisions for a given patient, then examined the hepatobiliary phase images for the same patient and also recorded the decisions they made on the basis of all MR images.

Statistical analysis

For assessment of inter-reader variability for image interpretation, the unweighted κ statistic was used to measure

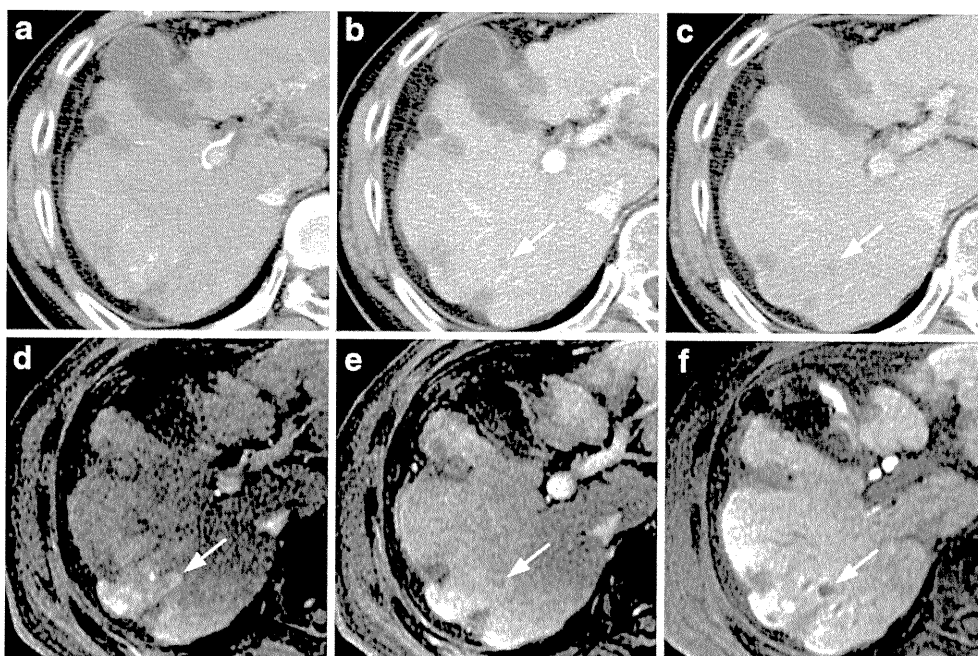


Fig. 2 HCC of a 60-year-old-man with hepatitis C cirrhosis, histologically proved at liver transplantation. CTHA revealed hypervascularity of the lesion (not shown). Contrast-enhanced CT image obtained during arterial dominant phase (**a**) does not show a hypervascular lesion in the right liver lobe, but images obtained during portal venous dominant (**b**) and equilibrium (**c**) phases show a nodule (*arrows*) with mild hypoattenuation compared with the surrounding liver parenchyma. Corresponding gadoxetic acid-enhanced MR image obtained during the arterial dominant (**d**) and portal venous dominant (**e**) phases show an 8-mm hypervascular nodule, which has become slightly hypoattenuating (*arrows*). On the MR image obtained during the hepatobiliary phase (20 min after contrast medium administration),

the lesion has become hypointense against the highly enhanced background liver parenchyma (**f**). All the readers assigned this lesion a confidence score of 0 on CT images because of a lack of arterial hypervascularity. On dynamic MR images alone, two readers assigned it a score of 2, one assigned it a score of 3, and the remaining two readers assigned it a score of 4. On combined dynamic and hepatobiliary phase MR images, one reader assigned the lesion a score of 3, while the remaining four readers assigned it a score of 4. The addition of the hepatobiliary phase to dynamic MR images increased the confidence level for this lesion, because the lesion was conspicuously delineated on the hepatobiliary phase images

the extent of agreement among the five readers regarding the presence (score 3 or 4) or absence (score 2 or less) of lesions. κ values of up to 0.40 were considered to indicate positive but poor agreement; 0.41–0.75, good agreement; and 0.75 or higher, excellent agreement [38].

Alternative free-response receiver operating characteristic (AFROC) analysis (ROCKIT 0.9B; C. E. Metz, University of Chicago, Chicago, IL, USA) was performed on a tumour-by-tumour basis [39]. The area under each AFROC curve, that is, the Az value, was used to indicate the overall diagnostic performance of each technique and each reader.

Sensitivity and positive predictive values for lesion detection with each technique for each reader were also determined by using only lesions assigned a confidence rating of 3 or 4.

Mean Az values, mean sensitivities and mean positive predictive values were compared among the various techniques by using the Scheffe post hoc test. Statistical analyses were performed for all lesions and for the subgroups of lesions with maximum diameters of less than 1 cm, 1–2 cm, and more than 2 cm. A *P* value of less than 0.05 was considered to indicate a statistically significant difference.

Results

Inter-reader agreement

The κ values for the five readers were 0.70 for multiphasic multidetector CT, 0.54 for dynamic MR imaging, and 0.55 for combined dynamic and hepatobiliary phase MR imaging. As for the presence of lesions, good agreement among the five readers was obtained for the detection of hypervascular HCC lesions with each of the techniques.

AFROC analysis

For all hypervascular HCC lesions and the subgroup of lesions 1 cm in diameter or smaller, the mean Az value, or diagnostic accuracy, for dynamic MR imaging alone or combined dynamic and hepatobiliary MR imaging was significantly higher than that for multiphasic multidetector CT (Table 2). For the subgroup of lesions 1–2 cm in diameter, there was no statistically significant difference among the techniques. In most instances, the Az value for the subgroup of lesions larger than 2 cm was degenerated because it was based on a data set with many tied values.

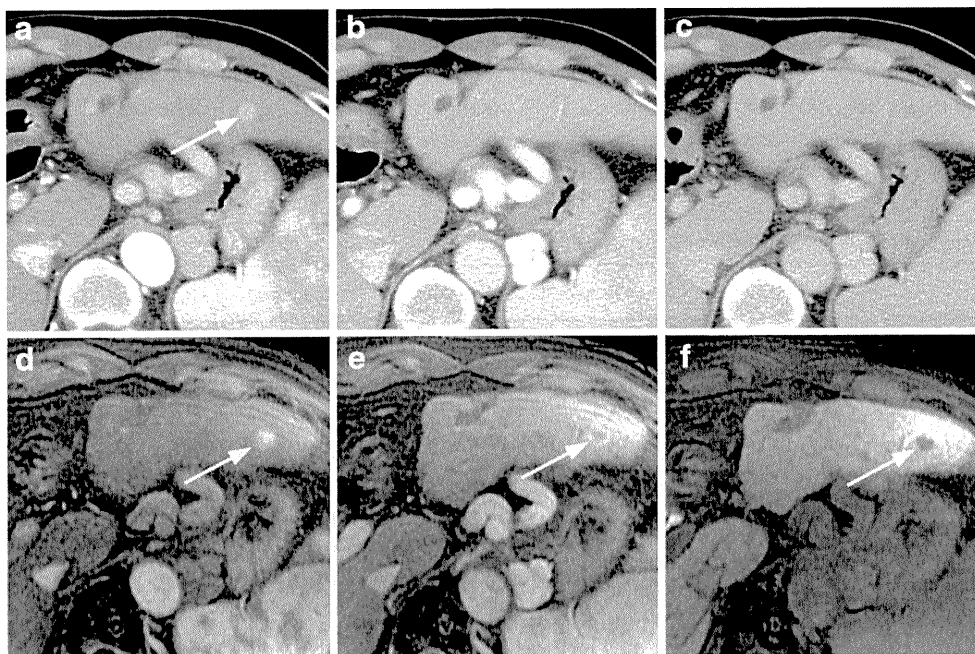


Fig. 3 Histologically proved HCC of a same patient as in Fig. 2. CTHA revealed hypervascularity of the lesion (not shown). Contrast-enhanced CT image obtained during the arterial dominant phase (a) shows a 10-mm hypervascular lesion in the left liver lobe (arrow), and images obtained during the portal venous dominant (b) and equilibrium (c) phases show isoattenuation compared with the surrounding liver parenchyma. The corresponding gadolinium-enhanced MR images obtained during the arterial dominant (d) and portal venous dominant (e) phases show a hypervascular nodule, which has become slightly hypointense (arrows). On the MR image obtained during

the hepatobiliary phase (20 min after contrast medium administration), the lesion has become hypointense against the highly enhanced background liver parenchyma (f). On dynamic MR images alone, three readers assigned the lesion a score of 2, one assigned it a score of 3 and one assigned it a score of 4. On combined dynamic and hepatobiliary phase MR images, three readers assigned the lesion a score of 3 and the remaining two readers a score of 4. On CT images, three readers assigned this lesion a confidence score of 2 because of a lack of “washout” enhancement pattern and the other two assigned it a confidence score of 3

Sensitivity

For all hypervascular HCC lesions and the subgroup of lesions 1 cm in diameter or smaller, the mean sensitivity for combined dynamic and hepatobiliary MR imaging was significantly higher than that for multiphase multidetector CT or dynamic MR imaging alone (Table 3, Fig. 2). For the subgroup of lesions 1–2 cm and 2 cm or more in diameter, the mean sensitivity for combined dynamic and hepatobiliary MR imaging was higher than that for multiphase multidetector CT or dynamic MR imaging alone, although the difference was not statistically significant (Fig. 3).

Four of the 73 lesions showed hyperintensity in comparison with the surrounding liver parenchyma on the hepatobiliary phase MR images. Another three lesions in three patients showed isointensity at the hepatobiliary phase and in two of these patients, the liver parenchyma demonstrated minimal enhancement at the hepatobiliary phase due to deterioration of liver function.

False-negative findings

Eight lesions (all ≤ 1 cm) of five patients, which were confirmed during hepatic transplantation ($n=3$) or angio-CT with imaging follow-up ($n=5$), were not detected with a high confidence score of 3 or 4 by any of the readers on any of the image sets.

In terms of specific image sets, 30 lesions (>2 cm, $n=2$; 1–2 cm, $n=7$; <1 cm, $n=21$) in 12 patients were not detected on CT images with high confidence by any of the readers. Of

these 30 lesions, 13 (>2 cm, $n=2$; 1–2 cm, $n=4$; <1 cm, $n=7$) in six patients were detected on dynamic MR images by at least one reader, while another nine lesions (1–2 cm, $n=2$; <1 cm, $n=7$) in eight patients were detected when hepatobiliary phase MR images were added to the dynamic MR images.

On gadoxetate disodium-enhanced dynamic MR images, 19 lesions (1–2 cm, $n=5$; <1 cm, $n=14$) in 10 patients were not detected with high confidence by any of the readers. Of these 19 lesions, nine (1–2 cm, $n=2$; <1 cm, $n=7$) in eight patients were detected when hepatobiliary phase MR images were added to the dynamic MR images and two lesions (1 cm, $n=2$) in two patients, which were not detected with combined dynamic and hepatobiliary phase MR images, were detected on CT images by at least one reader.

On combined dynamic and hepatobiliary phase MR images, eleven lesions (1–2 cm, $n=3$; <1 cm, $n=8$) in five patients were not detected with high confidence by any of the readers.

False-positive findings and positive predictive value

There were no significant differences between the mean positive predictive values for all three techniques (Table 4).

The false-positive lesions rated on CT images were retrospectively determined to be two arterial enhancing pseudolesion such as arterial-portal venous shunts (Fig. 4) and a regenerative nodule with mild atypia (histopathologically proven by biopsy). The actual numbers of false-positive lesions were 1, 1, 1, 1 and 2 for each reader, respectively, on CT images.

Table 4 Positive predictive values in the detection of hypervascular HCC

	Reader 1	Reader 2	Reader 3	Reader 4	Reader 5	Mean
All lesions ($n=73$)						
Multiphase CT	0.96 (27/28)	0.97 (29/30)	0.98 (39/40)	0.96 (26/27)	0.95 (41/43)	0.96
Dynamic MR imaging	0.91 (30/33)	0.95 (39/41)	0.94 (44/47)	0.97 (33/34)	0.98 (43/44)	0.95
Combined dynamic and hepatobiliary phase MR imaging	0.94 (49/52)	0.88 (46/52)	0.94 (46/49)	0.98 (52/53)	0.93 (53/57)	0.94
Lesions <1.0 cm ($n=28$)						
Multiphase CT	0.67 (2/3)	1.00 (2/2)	1.00 (5/5)	N/A (0/0)	0.86 (6/7)	0.88
Dynamic MR imaging	0.75 (3/4)	1.00 (8/8)	1.00 (10/10)	1.00 (4/4)	1.00 (8/8)	0.95
Combined dynamic and hepatobiliary phase MR imaging	0.93 (13/14)	0.75 (12/16)	1.00 (12/12)	1.00 (16/16)	0.88 (14/16)	0.91
Lesions 1.0–2.0 cm ($n=32$)						
Multiphase CT	1.00 (14/14)	0.94 (16/17)	0.96 (23/24)	0.94 (15/16)	0.96 (24/25)	0.96
Dynamic MR imaging	0.88 (15/17)	0.90 (19/21)	0.92 (22/24)	0.95 (18/19)	0.96 (23/24)	0.92
Combined dynamic and hepatobiliary phase MR imaging	0.92 (23/25)	0.92 (22/24)	0.92 (22/24)	0.96 (26/27)	0.93 (27/29)	0.93
Lesions >2.0 cm ($n=13$)						
Multiphase CT	1.00 (11/11)	1.00 (11/11)	1.00 (11/11)	1.00 (11/11)	1.00 (11/11)	1.00
Dynamic MR imaging	1.00 (11/11)	1.00 (12/12)	0.92 (12/13)	1.00 (9/9)	1.00 (12/12)	0.98
Combined dynamic and hepatobiliary phase MR imaging	1.00 (13/13)	1.00 (12/12)	0.92 (12/13)	1.00 (10/10)	1.00 (12/12)	0.98

Numbers in parentheses are actual numbers of lesions. Regardless of lesion size, there were no statistically significant differences among the imaging techniques

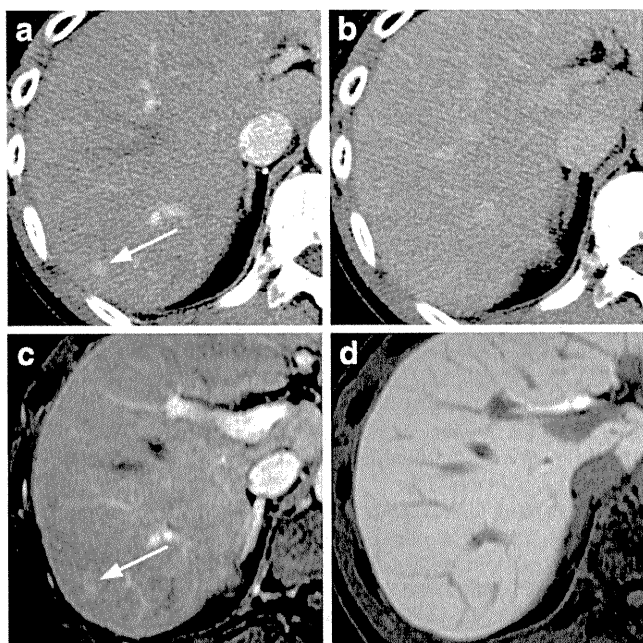


Fig. 4 Images of hepatitis B cirrhosis in a 68-year-old-man. Contrast-enhanced CT image obtained during the arterial dominant phase (a) shows a mildly enhanced lesion, 8 mm in diameter, in the right liver lobe (arrow), which has become isoattenuating during the equilibrium phase compared with the surrounding liver parenchyma (b). Corresponding gadolinic acid-enhanced MR image obtained during the arterial dominant phase (c) shows a lesion 8 mm in diameter with slight enhancement (arrow). The MR image obtained during the hepatobiliary phase (20 min after contrast-medium administration), shows that the lesion has become isointense compared with the surrounding liver parenchyma (d). On CT images, one reader assigned this lesion a confidence score of 0, one assigned it a score of 1, two assigned it a score of 2 and one a score of 4. On both dynamic MR images alone and combined dynamic and hepatobiliary phase MR images, all the readers assigned it a score of 0. On CTAP images, this lesion did not show a perfusion defect, and on follow-up CT images obtained 3 months later, the hyperattenuation observed during the arterial dominant phase was not seen. This lesion was therefore considered to be an arterial enhancing pseudolesion

The false-positive lesions rated on dynamic MR images alone and on combined dynamic and hepatobiliary phase MR images were retrospectively determined to be five small arterial enhancing pseudolesion, fibrotic change, and a regenerative nodule with mild atypia. Additionally, two small hepatic hemangiomas were assigned a score of 3 by one or two readers on combined dynamic and hepatobiliary phase MR images. The actual numbers of false-positive lesions were 3, 2, 3, 1 and 1 on dynamic MR images alone and 3, 6, 3, 1 and 4 on combined dynamic and hepatobiliary phase MR images.

Discussion

Previous studies [23, 24] have reported that gadolinic acid-enhanced MR imaging and multiphasic multi-

detector CT produce a similar diagnostic performance (A_z) for the detection of HCC using AFROC analysis. Our study demonstrated that, compared with multiphasic multidetector CT, gadolinic acid-enhanced MR imaging including dynamic and hepatobiliary phase imaging significantly improved not only the sensitivity but also the diagnostic accuracy for the detection of hypervascular HCC. One of the reasons for this difference may be that the size of the tumours examined in our study was smaller than that of tumours examined in previous studies. Statistical analyses of the subgroups classified by lesion size showed that only for the subgroup of lesions 1 cm in diameter or smaller, the mean A_z for combined dynamic and hepatobiliary MR imaging was significantly higher than that for multiphasic multidetector CT. Meanwhile, there were no significant differences among the techniques in the detection lesions 1 cm in diameter or larger.

Since, at the recommended dosage, the amount of gadolinium in gadolinic acid disodium medium is only one-fourth that in conventional extracellular gadolinium chelates medium, dynamic MR imaging using gadolinic acid may show weaker enhancement than that using extracellular medium [31]. This might impair the sensitivity for detection of hypervascular HCC due to weaker tumour enhancement at the arterial dominant phase or compromise the characterisation of the lesions based on lesion vascularity. However, our study, which evaluated the diagnostic accuracy of HCC by taking tumour vascularity into consideration, demonstrated that sensitivity for the detection of hypervascular HCC on gadolinic acid-enhanced dynamic MR images without hepatobiliary images was higher than that for multiphasic multidetector CT, although the difference was not statistically significant, and that the diagnostic accuracy (A_z) of gadolinic acid-enhanced dynamic MR imaging was significantly higher than that of CT. The use for dynamic imaging of a three-dimensional gradient-echo sequence dedicated to liver imaging (e.g. LAVA or THRIVE) may enhance MR imaging.

The addition of hepatobiliary phase images to dynamic images improved sensitivity for the detection of hypervascular HCC. However, more false-positive findings were identified on combined dynamic and hepatobiliary phase MR images than on dynamic images. Two small hemangiomas and an arterial enhancing pseudolesion were additionally classified as hypervascular HCCs by one or two readers on combined MR images. A previous study reported that high-flow hepatic hemangioma on gadolinic acid-enhanced MR imaging mimicked hypervascular tumour due to “pseudo washout” sign [40]. Another study reported that a small proportion of arterial enhancing pseudolesions demonstrated low signal intensity on hepatobiliary phase [41]. This may also result in the false-positive lesions.

Analyses of inter-reader variability demonstrated slightly lower agreement at MR imaging (both dynamic and combined images) compared to that at CT, although good agreement was obtained with each technique. This may be thought to be causally related to the complexity of diagnosis using various image contrasts and extended criteria for diagnosing HCC at MR imaging.

The present study has certain limitations. First, our study is a retrospective study and our study population was not a surveillance population. All patients were suspected of having at least one possible HCC nodule and underwent CT arterial portography, CT hepatic arteriography for transarterial chemoembolisation or evaluation before surgical resection. Selection bias may have resulted in an overestimation of the actual diagnostic performance because of the exclusion of negative imaging studies. Secondly, as in the case with some previous studies [22, 24, 42], a potential limitation of our study could be the lack of histologic proof for some HCCs. However, several kinds of confirmatory findings were available, including those obtained with CTAP, CTHA and follow-up CT or follow-up MR imaging. Thirdly, our study population size of 31 was rather small, so that, with a larger patient population, our data could have achieved more robust statistical significance. Inally, at CT examination, an 8-channel CT was used for some patients; the use of 64-channel CT for these patients may improve the diagnostic performance at CT.

In summary, our results demonstrate that, compared with multiphase multidetector CT, gadoxetate disodium-enhanced MR imaging including dynamic and hepatobiliary phase images results in significantly improved sensitivity and diagnostic accuracy for the detection of hypervascular HCC.

Acknowledgements This work was supported in part by a Grant-in-Aid for Young Scientists (21791191) from the Ministry of Education, Culture, Sports, Science and Technology and by Health and Labor Sciences Research Grants (KAKENHI), Japan Society for the Promotion of Science.

References

- Bruix J, Sherman M (2005) AASLD practice guideline: management of hepatocellular carcinoma. *Hepatology* 42:1208–1236
- Bruix J, Sherman M (2011) AASLD practice guideline: management of hepatocellular carcinoma: an update. *Hepatology* 53:1020–1022
- Bruix J, Sherman M, Llovet JM et al (2001) Clinical management of hepatocellular carcinoma: conclusions of the Barcelona-2000 EASL conference. *J Hepatol* 35:421–430
- Torzilli G, Minagawa M, Takayama T et al (1999) Accurate preoperative evaluation of liver mass lesions without fine-needle biopsy. *Hepatology* 30:889–893
- Levy I, Greig PD, Gallinger S et al (2001) Resection of hepatocellular carcinoma without preoperative tumour biopsy. *Ann Surg* 234:206–209
- Schuhmann-Giampieri C, Schmitt-Willich H, Press WR et al (1992) Preclinical evaluation of Gd-EOB-DTPA as a contrast agent in MR imaging of the hepatobiliary system. *Radiology* 183:59–64
- Clement O, Mühler A, Vexler V et al (1992) Gadolinium-ethoxybenzyl-DTPA: a new liver-specific magnetic resonance contrast agent-kinetic and enhancement patterns in normal and cholestatic rats. *Invest Radiol* 27:612–619
- Mühler A, Clément O, Saeed M et al (1993) Gadolinium-ethoxybenzyl-DTPA: a new liver-directed magnetic resonance contrast agent-absence of acute epatotoxic, cardiovascular, or immunologic effects. *Invest Radiol* 28:26–32
- Weinmann HJ, Schuhmann-Gampieri G, Schmitt-Willich H et al (1991) A new lipophilic gadolinium chelate as a tissue-specific contrast medium for MRI. *Magn Reson Med* 22:222–228
- Muehler A HI, Weinmann HJ (1994) Elimination of Gd-EOB-DTPA in severely impaired liver and kidney excretory function. *Invest Radiol* 29:213–216
- Kitao A, Matsui O, Yoneda N et al (2011) The uptake transporter OATP8 expression decreases during multistep hepatocarcinogenesis: correlation with gadoxetic acid enhanced MR imaging. *Eur Radiol* 21:2056–2066
- Reimer P, Schneider G, Schima W (2004) Hepatobiliary contrast agents for contrast-enhanced MRI of the liver: properties, clinical development and applications. *Eur Radiol* 14:559–578
- Reimer P, Rummeny EJ, Shamsi K et al (1996) Phase II clinical evaluation of Gd-EOB-DTPA: dose, safety aspects and pulse sequence. *Radiology* 199:177–183
- Golfieri R, Renzulli M, Lucidi V, Corcioni B, Trevisani F, Bolondi L (2011) Contribution of the hepatobiliary phase of Gd-EOB-DTPA-enhanced MRI to Dynamic MRI in the detection of hypovascular small (≤ 2 cm) HCC in cirrhosis. *Eur Radiol* 21:1233–1242
- Löwenthal D, Zeile M, Lim WY et al (2011) Detection and characterisation of focal liver lesions in colorectal carcinoma patients: comparison of diffusion-weighted and Gd-EOB-DTPA enhanced MR imaging. *Eur Radiol* 21:832–840
- Shimada K, Isoda H, Hirokawa Y, Arizono S, Shibata T, Togashi K (2010) Comparison of gadolinium-EOB-DTPA-enhanced and diffusion-weighted liver MRI for detection of small hepatic metastases. *Eur Radiol* 20:2690–2698
- Ricke J, Thormann M, Ludewig M et al (2010) MR-guided liver tumour ablation employing open high-field 1.0T MRI for image-guided brachytherapy. *Eur Radiol* 20:1985–1993
- Choi JS, Kim MJ, Choi JY, Park MS, Lim JS, Kim KW (2010) Diffusion-weighted MR imaging of liver on 3.0-Tesla system: effect of intravenous administration of gadoxetic acid disodium. *Eur Radiol* 20:1052–1060
- Tanimoto A, Lee JM, Murakami T, Huppertz A, Kudo M, Grazioli L (2009) Consensus report of the 2nd International Forum for Liver MRI. *Eur Radiol* 19:S975–S989
- Zech CJ, Grazioli L, Jonas E et al (2009) Health-economic evaluation of three imaging strategies in patients with suspected colorectal liver metastases: Gd-EOB-DTPA-enhanced MRI vs. extracellular contrast media-enhanced MRI and 3-phase MDCT in Germany, Italy and Sweden. *Eur Radiol* 19:S753–S763
- Reimer P, Rummeny EJ, Daldrup HE et al (1997) Enhancement characteristics of liver metastases, hepatocellular carcinomas, and hemangiomas with Gd-EOB-DTPA: preliminary results with dynamic MR imaging. *Eur Radiol* 7:275–280
- Ichikawa T, Saito K, Yoshioka N et al (2010) Detection and characterization of focal liver lesions: a Japanese phase III, multicenter comparison between gadoxetic acid disodium-enhanced magnetic resonance imaging and contrast-enhanced computed tomography predominantly in patients with hepatocellular carcinoma and chronic liver disease. *Invest Radiol* 45:133–141

23. Kim SH, Kim SH, Lee J et al (2009) Gadoteric acid-enhanced MRI versus triple-phase MDCT for the preoperative detection of hepatocellular carcinoma. *AJR Am J Roentgenol* 192:1675–1681
24. Kim YK, Kim CS, Han YM et al (2009) Detection of hepatocellular carcinoma: gadoteric acid-enhanced 3-dimensional magnetic resonance imaging versus multi-detector row computed tomography. *J Comput Assist Tomogr* 33:844–850
25. Hammerstingl R, Huppertz A, Breuer J et al (2008) Diagnostic efficacy of gadoteric acid (Primovist)-enhanced MRI and spiral CT for a therapeutic strategy: comparison with intraoperative and histopathologic findings in focal liver lesions. *Eur Radiol* 18:457–467
26. Halavaara J, Breuer J, Ayuso C et al (2006) Liver tumour characterization: comparison between liver-specific gadoteric acid disodium-enhanced MRI and biphasic CT—a multicenter trial. *J Comput Assist Tomogr* 30:345–354
27. Huppertz A, Balzer T, Blakeborough A et al (2004) Improved detection of focal liver lesions at MR imaging: multicenter comparison of gadoteric acid-enhanced MR images with intraoperative findings. *Radiology* 230:266–275
28. Huppertz A, Haraida S, Kraus A et al (2005) Enhancement of focal liver lesions at gadoteric acid-enhanced MR imaging: correlation with histopathologic findings and spiral CT-initial observations. *Radiology* 234:468–478
29. Vogl TJ, Kümmel S, Hammerstingl R et al (1996) Liver tumours: comparison of MR imaging with Gd-EOB-DTPA and Gd-DTPA. *Radiology* 200:59–67
30. Bluemke DA, Sahani D, Amendola M et al (2005) Efficacy and safety of MR imaging with liver-specific contrast agent: U.S. multicenter phase III study. *Radiology* 237:89–98
31. Akai H, Kiryu S, Takao H et al (2009) Efficacy of double-arterial phase gadolinium ethoxybenzyl diethylenetriamine pentaacetic acid-enhanced liver magnetic resonance imaging compared with double-arterial phase multi-detector row helical computed tomography. *J Comput Assist Tomogr* 33:887–892
32. Murakami T, Takamura M, Kim T et al (2005) Double phase CT during hepatic arteriography for diagnosis of hepatocellular carcinoma. *Eur J Radiol* 54:246–252
33. Iannaccone R, Laghi A, Catalano C et al (2005) Hepatocellular carcinoma: role of unenhanced and delayed phase multi-detector row helical CT in patients with cirrhosis. *Radiology* 234:460–467
34. Hayat MA (2009) Methods of cancer diagnosis, therapy, and prognosis. Volume 5, Liver Cancer. Springer, New York, pp 221–235
35. Murakami T, Kim T, Takamura M et al (2001) Hypervascular hepatocellular carcinoma: detection with double arterial phase multi-detector row helical CT. *Radiology* 218:763–767
36. Tsuboyama T, Onishi H, Kim T et al (2010) Hepatocellular carcinoma: hepatocyte-selective enhancement at gadoteric acid-enhanced MR imaging—correlation with expression of sinusoidal and canalicular transporters and bile accumulation. *Radiology* 255:824–833
37. Kogita S, Imai Y, Okada M et al (2010) Gd-EOB-DTPA-enhanced magnetic resonance images of hepatocellular carcinoma: correlation with histological grading and portal blood flow. *Eur Radiol* 20:2405–2413
38. Fleiss JL (1981) The measurement of interrater agreement. In *Statistical methods for rates and proportions*. 2nd ed., Wiley, New York, pp 212–236
39. Chakraborty DP, Winter LH (1990) Free-response methodology: alternate analysis and a new observer-performance experiment. *Radiology* 174:873–881
40. Doo KW, Lee CH, Choi JW et al (2009) “Pseudo washout” sign in high-flow hepatic hemangioma on gadoteric acid contrast-enhanced MRI mimicking hypervascular tumour. *Am J Roentgenol* 193: W490–496
41. Sun HY, Lee JM, Shin CI et al (2010) Gadoteric acid-enhanced magnetic resonance imaging for differentiating small hepatocellular carcinomas (2 cm in diameter) from arterial enhancing pseudolesions: special emphasis on hepatobiliary phase imaging. *Invest Radiol* 45:96–103
42. Marin D, Di Martino M, Guerrisi A et al (2009) Hepatocellular carcinoma in patients with cirrhosis: qualitative comparison of gadobenate dimeglumine-enhanced MR imaging and multiphase 64-section CT. *Radiology* 251:85–95

Focal Nodular Hyperplasia-Like Nodule with Reduced Expression of Organic Anion Transporter 1B3 in Alcoholic Liver Cirrhosis

Nobuko Doi¹, Yasuyuki Tomiyama¹, Tomoya Kawase¹, Sohji Nishina¹, Naoko Yoshioka¹, Yuichi Hara¹, Koji Yoshida¹, Keiko Korenaga¹, Masaaki Korenaga¹, Takuya Moriya², Atsushi Urakami³, Osamu Nakashima⁴, Masamichi Kojiro⁴ and Keisuke Hino¹

Abstract

We report a patient with alcoholic liver cirrhosis who had a 15 mm focal nodular hyperplasia (FNH)-like nodule in the liver. This FNH-like nodule was diagnosed as hepatocellular carcinoma (HCC) mainly based on hypervascularity during the hepatic arterial phase, washout pattern during the equilibrium phase and low signal intensity during the hepatobiliary phase in gadolinium-ethoxybenzyl-diethylenetriamine pentaacetic acid (Gd-EOB-DTPA)-enhanced MRI; it was surgically resected. Its histology exhibited hepatocyte hyperplasia, fibrous septa containing unpaired small arteries accompanied by reactive bile ductules, remarkable iron deposits and sinusoidal capillarization, and was compatible with the diagnosis of an FNH-like nodule. When we analyzed the images of the present nodule retrospectively, low signal intensity on in-phase and isosignal intensity on opposed-phase T1-weighted MRI may have reflected iron deposits in the FNH-like nodule. In addition, a low signal intensity on T2-weighted MRI and no detection in diffusion-weighted MRI may help in distinguishing FNH-like nodules from HCC, since these image findings are inconsistent with typical HCC. Immunohistochemical analysis revealed a markedly reduced expression of organic anion transporter (OATP) 1B3 in this nodule, which implied decreased Gd-EOB-DTPA uptake by hepatocytes and accounted for the low signal intensity during the hepatobiliary phase on Gd-EOB-DTPA-enhanced MRI. To the best of our knowledge this is the first report in which an FNH-like nodule was assessed for OATP1B3 expression.

Key words: alcoholic liver cirrhosis, FNH-like nodule, hepatocellular carcinoma, organic anion transporter, Gd-EOB-DTPA-enhanced MRI

(Intern Med 50: 1193-1199, 2011)

(DOI: 10.2169/internalmedicine.50.4637)

Introduction

Due to improvements in imaging techniques and pathological evaluation, a new type of small focal lesion occurring in the cirrhotic liver has been described (1-3). Focal nodular hyperplasia (FNH)-like nodules (FNH-like nodules) are focal lesions occurring in liver cirrhosis and are morphologically very similar to classical FNH in the otherwise nor-

mal liver. In general, FNH-like nodules are assumed not to have an increased risk of malignant transformation (1-3), but this issue remains elusive (4). FNH-like nodules are occasionally misdiagnosed on imaging as hepatocellular carcinoma (HCC) due to hypervascularity during the arterial phase of magnetic resonance imaging (MRI)/computed tomography (CT).

On the other hand, gadolinium-ethoxybenzyl-diethylenetriamine pentaacetic acid (Gd-EOB-DTPA)-

¹Departments of Hepatology and Pancreatology, Kawasaki Medical University, Japan, ²Department of Pathology, Kawasaki Medical University, Japan, ³Department of Digestive Surgery, Kawasaki Medical University, Japan and ⁴Department of Pathology, Kurume University School of Medicine, Japan

Received for publication October 5, 2010; Accepted for publication December 17, 2010

Correspondence to Dr. Keisuke Hino, khino@med.kawasaki-m.ac.jp

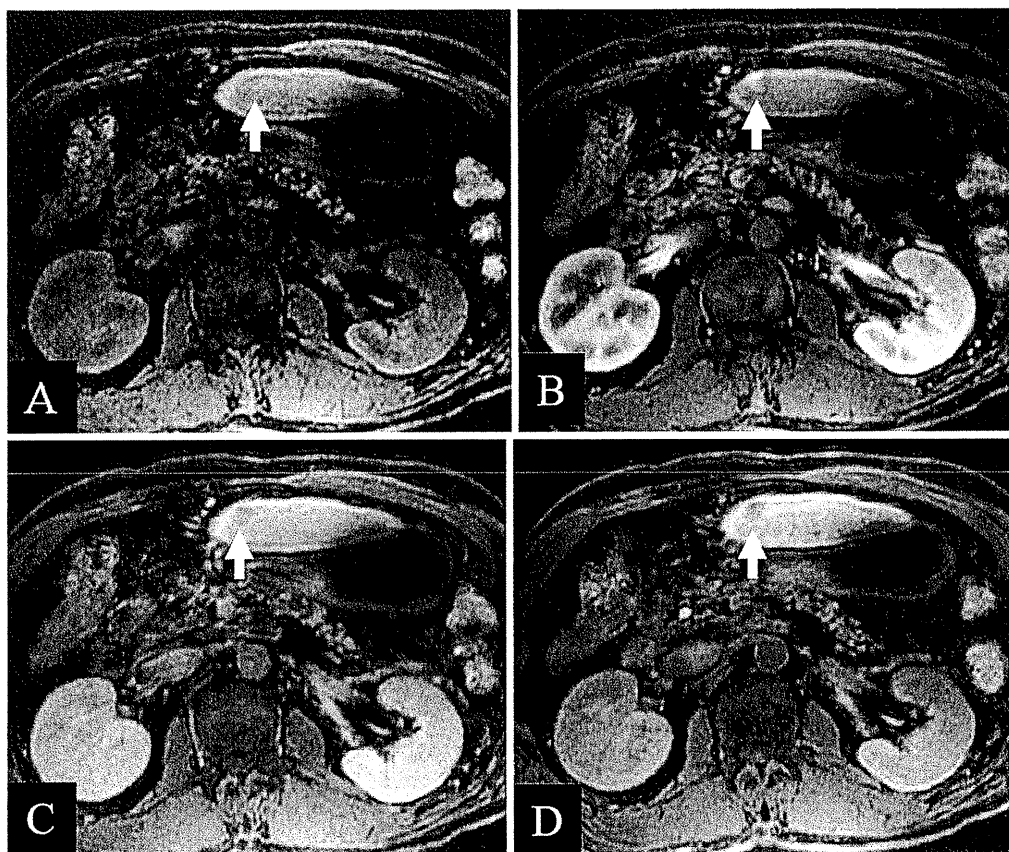


Figure 1. Images of the FNH-like nodule in segment 3 in Gd-EOB-DTPA-enhanced MRI. Arrows indicate a 9mm FNH-like nodule. (A) Low signal intensity before contrast injection, (B) High signal intensity during the hepatic arterial phase, (C) Washout pattern during the equilibrium phase, (D) Low signal intensity during the hepatobiliary phase.

enhanced MRI has enabled us to detect focal liver lesions because of its hepatocyte-specific properties (5-7), and it might be the most useful imaging modality for the diagnosis of HCC at present (8, 9). However, the image findings of FNH-like nodules in Gd-EOB-DTPA-enhanced MRI are not well known, and it remains unclear if FNH-like nodules can be distinguished from HCC in Gd-EOB-DTPA-enhanced MRI. Here, we report a histologically proven FNH-like nodule in a patient with alcoholic liver cirrhosis, and discuss the diagnostic potential of Gd-EOB-DTPA-enhanced MRI for FNH-like nodules.

Case Report

A 68-year-old Japanese man with a history of alcoholic liver cirrhosis for approximately 10 years was found to have a 9 mm hypervascular nodule in the liver through contrast-enhanced CT and admitted to Kawasaki Medical University Hospital in June 2008 for further examination of the hepatic nodule.

His alcoholic consumption over the previous 40 years was 100 g or more per day. A physical examination on admission showed no remarkable abnormalities except for moderate splenomegaly. Laboratory data on admission disclosed

the following abnormal values: platelet count $9.4 \times 10^4 / \mu\text{L}$ (normal range 15-35), aspartate aminotransferase 58 IU/L (10-35), γ -glutamyl transpeptidase 346 IU/L (5-60) and indocyanine green retention rate at 15 minutes 16.4% (<10). The levels of hepatic tumor markers were as follows: α -fetoprotein 9.0 ng/mL (<10) and des- γ -carboxy prothrombin 25 mAU/mL (<40). The serum was negative for anti-hepatitis C virus antibody and hepatitis B surface (HBs) antigen but positive for anti-HBs and anti-hepatitis B core antibodies.

Neither B-mode sonographic scans nor Sonazoid contrast-enhanced ultrasonography detected the hepatic nodule. Arteriography did not disclose any hypervascular mass lesion. Contrast-enhanced CT revealed a nodule of 9 mm in the liver segment 3 as hypervascularity during the hepatic arterial phase. Gd-EOB-DTPA-enhanced MRI disclosed that this nodule had a low signal intensity before contrast injection (Fig. 1A), hypervascularity during the hepatic arterial phase (Fig. 1B), a washout pattern during the equilibrium phase (Fig. 1C), and a low signal intensity during the hepatobiliary phase (Fig. 1D). Diffusion-weighted MRI did not reveal this nodule (Fig. 2A). In- and opposed-phase T1-weighted MRI, and T2-weighted MRI disclosed this nodule as low signal intensity (Fig. 2B), isosignal intensity (Fig. 2C) and slightly